



Investigations on sheet metal forming of hybrid parts in different stress states

Jan Hafenecker^{1,2} · Marion Merklein^{1,2}

Received: 21 October 2022 / Accepted: 16 November 2022 / Published online: 24 November 2022
© The Author(s) 2022

Abstract

Conventional processes are being pushed to their limits by growing demands in terms of sustainability and diversity of variants. Hybrid components, which are produced by a combination of two or more manufacturing processes, are a suitable way of meeting these challenges. The combination of sheet metal forming processes with additive manufacturing offers the potential to link personalized components with standardized parts. Knowing that the additively manufactured components influence the forming process, it is essential to understand the interactions in detail. Therefore, this work will compare the influence of several additively manufactured elements (AME) for deep drawing with two different punch geometries. The approach used combines experimental and numerical investigations to improve process insight in relation to sheet metal forming of hybrid components. The results show that the AMEs amplify existing stresses and strains in dependence of the present load. Sections subjected to low loads, as it is found in the bottom of the cup manufactured with a cylindrical punch, are hardly affected, whereas stronger loaded areas, e.g. the center of the parts manufactured with a hemispherical punch, are affected all the more.

Keywords Additive manufacturing · Powder bed fusion · Hybrid · Sheet metal forming · FEM · 316L

1 Introduction

The ongoing goal upon improving customers' satisfaction with products and services, which are closer to their needs, while at the same time producing at mass production efficiency, is called mass customization [1]. The customization itself can appear in every of the four common operational activities (design, fabrication, assembly, distribution) of a manufacturing company [2], shown in Fig. 1.

The amount of possible standardization decreases for the integration of customization [3]. As a consequence, the amount of adaptations that have to be made and the complexity of the manufacturing process increase. For this reason, customization is nowadays mainly found in the step

“assembly” (Fig. 1b). For instance, choosing the color of a product. Additive manufacturing (AM) on the other hand offers the possibility to bring customization to the step “fabrication” and thus increases the amount of customization drastically (Fig. 1c). The tool-less approach makes it possible to build geometries impossible for other manufacturing techniques [4], e.g. lattice structures and cooling channels. At the same time, AM offers a maximum of flexibility [5]. The functionality of the parts can be increased [5] and the materials are used in an efficient way [4]. However, long production times keep AM from mass production productivity [4]. Furthermore, additively manufactured parts often require post-treatments, e.g. heat treatments [6] and machining [7], or else material defects, rough surfaces and low ductility can deteriorate the fatigue performance of the parts [8]. As mentioned before, with the earlier appearance of customization, the complexity of the process increases and the amount of standardization decreases. For instance, this is visible for the machining of additively manufactured parts, as the elaborate geometry of AM parts makes them hard to fix [4]. To reduce the complexity of production sequences including additive technologies, hybridization, i.e. a combination of manufacturing techniques, is used

✉ Jan Hafenecker
jan.hafenecker@fau.de

¹ Institute of Manufacturing Technology, Friedrich-Alexander-Universität Erlangen-Nürnberg, Egerlandstraße 13, 91058 Erlangen, Germany

² Collaborative Research Center 814-Additive Manufacturing, Am Weichselgarten 10, 91058 Erlangen-Tennenlohe, Germany

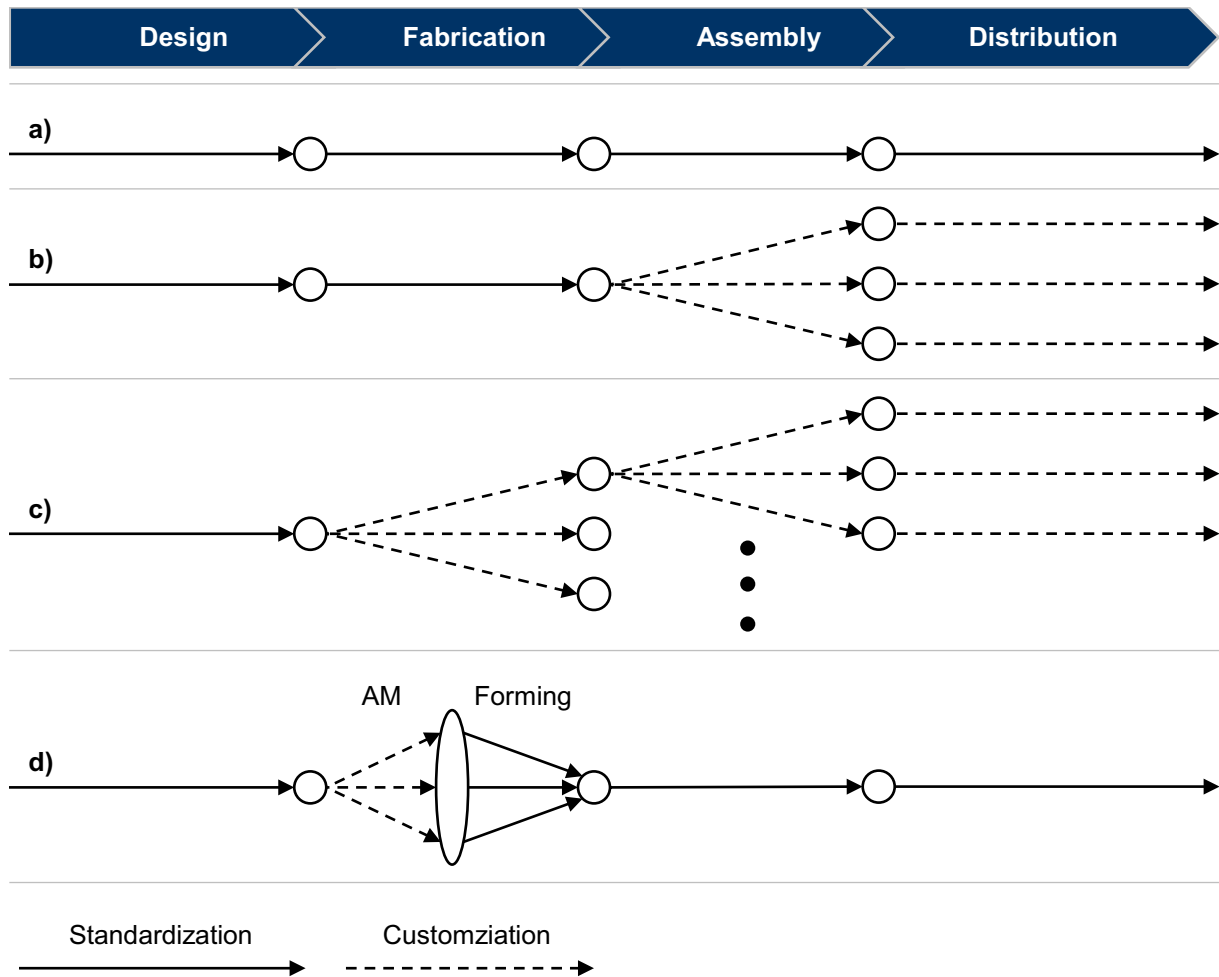


Fig. 1 Four operational activities of a manufacturing company according to [2] with different amounts of customization: **a** standardized process, **b** customization in assembly step, **c** customization in fabrication step, **d** hybridization in the fabrication step

(Fig. 1d). Hybrid processes in general expand the borders of single processes [9]. Hybrid processes including AM can thus overcome limitations such as low productivity, surface qualities and geometrical precision [10]. The combination of the processes can be at the same time and working zone [11] or sequential even without interactions between the processes [12]. Hybrid processes combining additive manufacturing and forming technologies developed drastically over the past years due to their beneficial synergies [10]. Forming technologies offer the production of parts with excellent mechanical and geometrical properties in mass production scale and costs [13] while AM technologies have the flexibility and geometrical freedom [7].

In [14], cups made of aluminum are deep drawn and material is added afterwards by directed energy deposition via laser beam (DED-LB/M) to increase the parts stiffness. If the material used is partly made of recycled powder, the energy demand for the production is lower compared to a conventional manufacturing with patchwork blanks.

Additionally, two strategies are pursued in [15]. In a first one, the coating strategy is chosen in a way that the thermal distortion is minimal. The second strategy aims at a minimal added mass. In both cases, the hybrid parts performance in terms of resistance to displacement under load is higher compared to conventionally manufactured counterparts. Selective laser sintering of stainless steels and single point incremental forming are used in [16]. Additive structures on sheet metal prior to the forming operation are used to build backing plates onto the sheet, increase the material thickness of the sheet and create complex geometries by the combination of AM and forming. The precision of the formed part was increased by the additive backing plates and the parts with the increase of material thickness resulted in lower thickness reductions compared to conventional sheet. The combination of both processes opened up the possibility to create geometries not feasible with the individual processes. Whole functional elements are built on sheet metal substrates and formed with a sheet bulk metal forming

operation in [17]. The resulting geometries are closer to the ideal final geometry than conventional sheet material and the hardness of the additive structures is higher than in the sheet metal as well. Still, there is an influence of the laser in the AM process on the mechanical properties of the sheet metal. This is also found in [18], where the authors used DED-LB/M to apply coatings to sheet metals before tensile and bending tests. The heat of the laser source is high enough to increase the grain size in the sheet metal substrate resulting in a reduction of strength and increase of ductility. For the authors in [19], an opposite effect is found. The coating of sheet metal substrate via DED-LB/M results in a reduced formability for the investigated tensile, stretch forming and Nakajima-tests. The starting point of failure by the means of cracking is found in the transition zone between additive layer and substrate material. This supports the assumption made by the authors in [20], that the manufacturing sequence of hybrid parts influences the formability. In detail, the additive structure is assumed to deteriorate the formability in terms of a stiffness increase. This is confirmed in [21] for the combination of powder bed fusion via laser beam (PBF-LB/M) and warm bending. The hybrid parts consisting of substrate sheet metal and additive functional elements failed prior to conventional sheet metal. In [22], the influence of a coating made by DED on the formability in a hole flanging test is investigated. Regardless of the side of the aluminum sheet metal, on which the layers are applied, the formability is reduced compared to the conventional parts due to the formation of brittle phases. The numerical approach of [23] predicted critical thickness reductions in the sheet metal of hybrid parts at the transition area to cylindrical additively manufactured functional elements (AME). An experimental validation to the results of the simulation is found for the same stretch forming operation in [24]. The presence of cylindrical additively manufactured elements on sheet metals in stretch forming operations leads to an earlier failure compared to conventional sheet metal. Furthermore, the same influence is found in other sheet metal forming operations but to different extents [25]. Stretch forming and bending operations with a single additively manufactured element

are more critical in terms of premature failure than deep drawing. Regarding the influence of AMEs on the forming operation different reasons can be found (Fig. 2): resistance towards the forming operation due to the geometry of the AME [23] and the gradient of mechanical properties [25], stress concentrations caused by sharp geometrical transitions and rough surfaces [25]. Investigations on the stress state present in the forming area are limited to [25], which is why further research is needed to fully understand the interactions between AMEs and the used sheet metal forming operation.

2 Methodology

In order to analyze the influence of the stress state on the forming of hybrid parts, within this investigation, a combination of numerical simulation and experimental approach is used. In a first step, the used finite element model is validated with experimental data. Secondly, the deep drawing process is investigated for two punch geometries [cylindrical punch (CP) and hemispherical punch (HP)] for plane sheet towards stress states and material flow. Additionally, critical areas are identified with the positioning of the AMEs in mind. Thirdly, the processes are performed with hybrid parts as simulations and physical experiments to see their influence. Based on that, the cause-effect relations are determined.

The investigated material is the stainless steel 316L (1.4404), which is often used in additive manufacturing and shows mechanical properties suitable for forming operations. The chemical composition of the sheet metal (Table 1a) and the powder material (Table 1b) are shown in Table 1. The thickness of the sheet metal is 1.5 mm and the powder particle size distribution is 19–43 μm.

The process sequence of hybrid parts manufactured by additive manufacturing and forming for this paper is described in the following Fig. 3. Sheet metal substrates with a thickness $t=1.5$ mm made of 316L are cut by laser. The functional elements are built on the sheet metal with powder

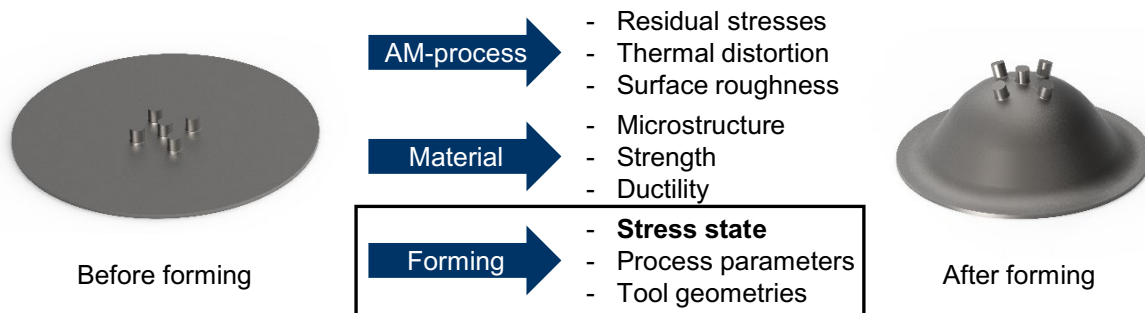


Fig. 2 Factors influencing the forming of hybrid parts

Table 1 Chemical composition of investigated sheet material (a) according to [26] and powder material (b) according to [27]

Ratio in wt%	C	Si	Mn	P	S	Cr	Mo	Ni	N	Fe
(a) Sheet metal										
Min	–	–	–	–	–	16.50	2.00	10.00	–	Bal.
Max	0.03	1.00	2.00	0.045	0.015	18.50	3.00	13.00	0.10	
(b) Powder material										
Min	–	–	–	–	–	16.00	2.00	10.00	–	Bal.
Max	0.03	1.00	2.00	0.045	0.015	18.00	3.00	14.00	0.10	

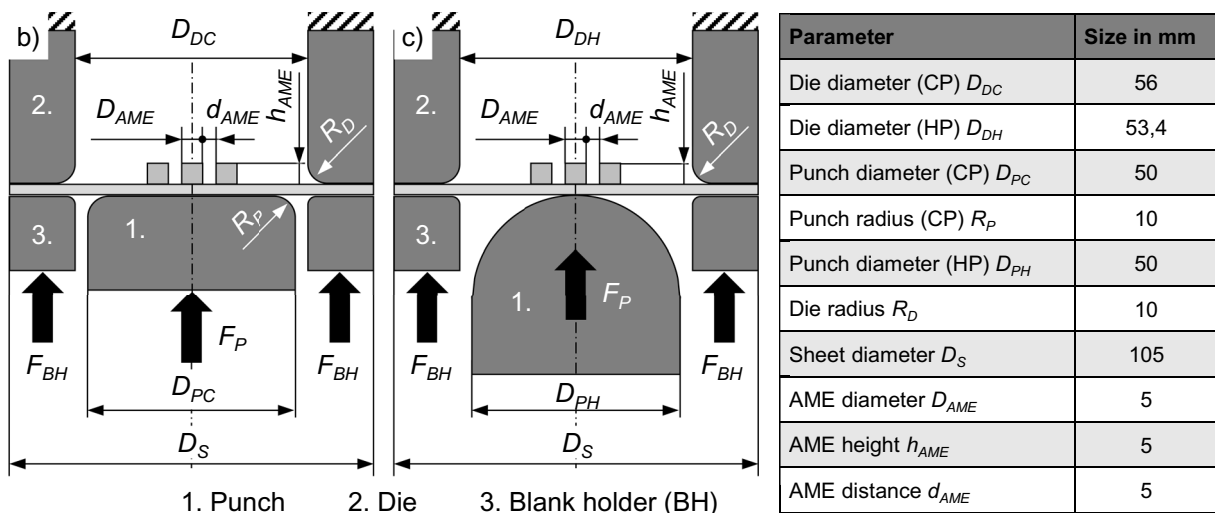
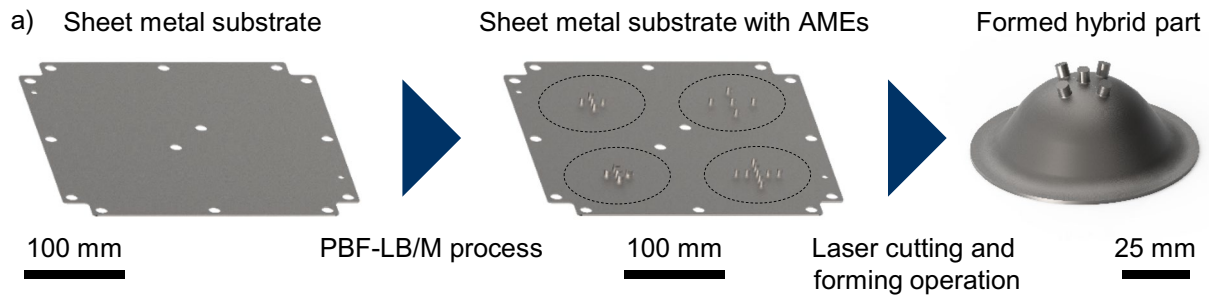


Fig. 3 a Process sequence to manufacture hybrid parts, tool dimensions for deep drawing with b cylindrical punch (CP) and c hemispherical punch (HP)

of the same material at a building platform temperature of 200 °C and with a volume energy of 127 J/mm³ using a LaserTec 30 SLM of the company DMG Mori. The substrate sheets with the functional elements built on it are then cut again by laser to manufacture the unformed hybrid parts with a diameter of 105 mm. The hybrid parts are formed at room temperature with a TSP 100 S0 hydraulic press of the company Lasco with the tools shown in Fig. 3b and c. Forming parameters are a punch displacement velocity v_p of 5 mm/s, a blank holder force F_{BH} of 25 kN and a fixed drawing depth d_d of 30 mm.

The optical measurement of the formed parts after the operation is done with an Atos Core 300 of the company

GOM GmbH. With that, geometry and thickness distribution can be measured and used to compare the physical parts with the results of the numerical simulations.

LS-Dyna (version mpp_d_R11_1) is used to calculate the results of the numerical forming processes. The setup of the numerical simulation is done according to [23]. Unlike in [23], the investigated material is the stainless steel 316L. Still, different material models can be assigned to each component of the hybrid part to match the differences in mechanical properties. The sheet is modelled using shell elements (Belytschko-Tsay with 9 integration points) and the material model “133-Barlat_YLD2000” based on [28], and the AME using constant stress solid elements and the material

model “024-PIECEWISE_LINEAR_PLASTICITY”. The material modelling is based on physical experiments. The true stress—true strain curves (Fig. 4) from uniaxial tensile tests at room temperature are approximated and extrapolated using the approach of Hockett-Sherby [29]. The heat input of the PBF-LB/M process on the sheet metal substrate is not considered in the numerical simulation. The tools are modelled with shell elements (Belytschko-Tsay 3 integration points) and the material model “020-RIGID”. The simulation is performed with quarter models to reduce the calculation time. With this in mind, additional boundary conditions are added at the edges (lateral and rotational constraints).

The different ways to compare the numerical simulation and experiment and also to investigate the influence of the stress state are shown in Fig. 5. For the comparison with the physical parts, the contour in and perpendicular to the rolling direction (RD) as well as the thickness distribution

and the thickness reduction are derived for sections. The thickness is derived in terms of distribution over the whole part as well. The contour is used to compare the geometry of the physical and numerical results. The thickness and its reduction are used for the identification of critical areas in terms of material failure by crack formation. The sections are preferably shown for the results in rolling direction, as this is the direction with lowest strength. Thus, the sheet thickness reduction is higher and a failure more likely to arise. Within the simulation, stress concentrations can be found, which can be an indicator for critical areas. Moreover, it is possible to identify the stress state of each element.

For the validation of the numerical model, simulations with and without AMEs are compared to the physical counterparts regarding geometry and force–displacement-curves. In a next step, the influence of stress state is investigated. Parts with and without AMEs are formed in a deep drawing

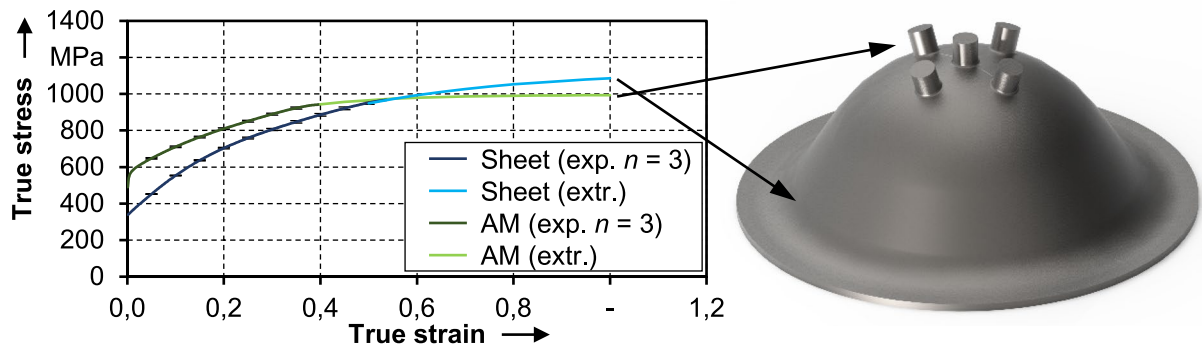


Fig. 4 True stress—true strain curves used for material modelling in the numerical simulation

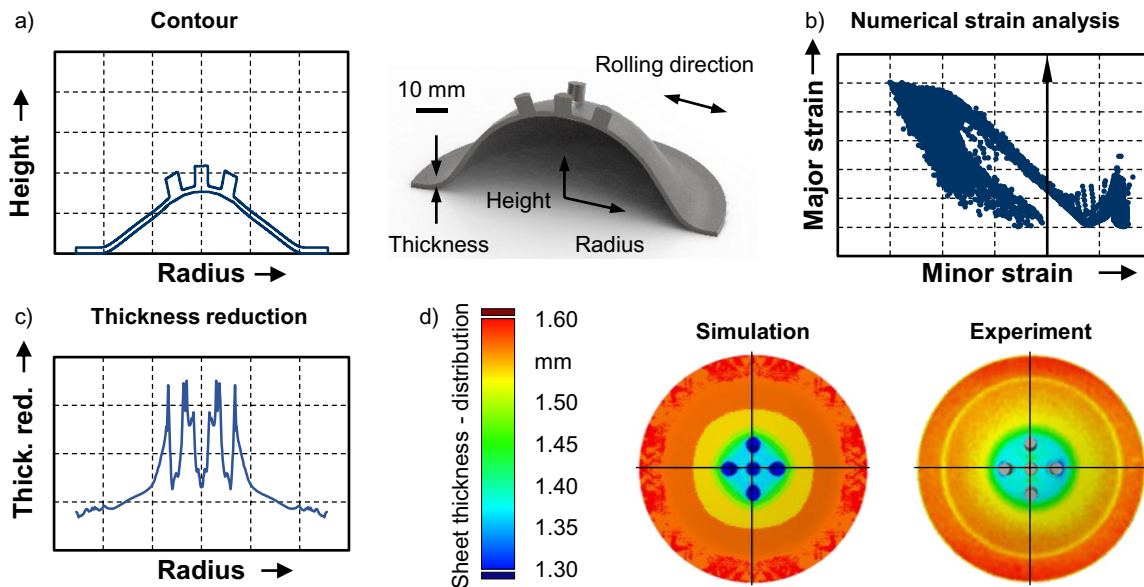


Fig. 5 Used analyses within this work: **a** contour of the hybrid part, **b** numerical strain analysis, **c** sheet thickness reduction along section, **d** sheet thickness distribution

operation with two punch geometries. By forming parts without AMEs the stress states and critical areas can be found for the conventional process. The results are used to work out the differences between the punch geometries but more importantly see the influence of the AMEs. Based on that, the influence of the stress state on the forming of hybrid parts can be derived.

3 Results and discussion

The results are separated into four parts. First, the numerical model of the forming processes is validated. Second, a comparison between the two processes for plane sheet is made. Third, the influence of the AMEs on each process is analyzed individually. In the end, the resulting influence of AMEs is compared for both processes.

3.1 Validation of the numerical model used for the forming simulation of hybrid parts

The validation of the numerical model used for the two forming processes is performed by comparing the contour of parts formed to the same drawing depth and the resulting force–displacement curves. The force–displacement curves for the two investigated punch geometries are shown in Fig. 6 for the plane sheet as well as for the hybrid part.

In general, the comparison between experiment and numerical simulation shows a good accordance. The highest deviations are found for the maximum force of the parts, formed with hemispherical punch. However, the deviations are comparably small, i.e. average deviations below 4 kN. Therefore, the accuracy is assumed to be sufficient. The high

accordance of the simulation's force–displacement curves to the physical experiments supports the validity of the material modelling approach and the setup of the numerical model. A second comparison is performed towards the geometry of the formed parts. Again, the results of the numerical simulation are compared with physical counterparts. Cross sections in rolling direction of the parts formed up to a drawing depth of 30 mm are shown in Fig. 7 for the two investigated tool geometries.

Regardless of the geometry, the accordance between physical experiments and numerical results is high. This can be seen for the forming processes with plane sheet, but in particular for the hybrid parts. At the functional elements, the thickness deviation of the sheet is clearly visible. Beneath the AME the thickness of the sheet is higher than in the surrounding area, creating a slightly convex shape. This is found for the numerical parts as well as for the physical parts. Due to the precise accordance between the geometries, the validity of the numerical model is additionally supported.

To summarize, the force–displacement curves and the comparison of the geometry in cross section show a high accordance between the numerical simulation and the physical experiments. Therefore, the numerical modelling of the forming processes with sheet and hybrid parts is validated and can be used to develop a deeper understanding of what happens during the forming operation.

3.2 Comparison of the stress/strain states between punch geometries

Deep drawing is a common processes in the field of sheet metal forming. Still, there is a difference regarding the stress

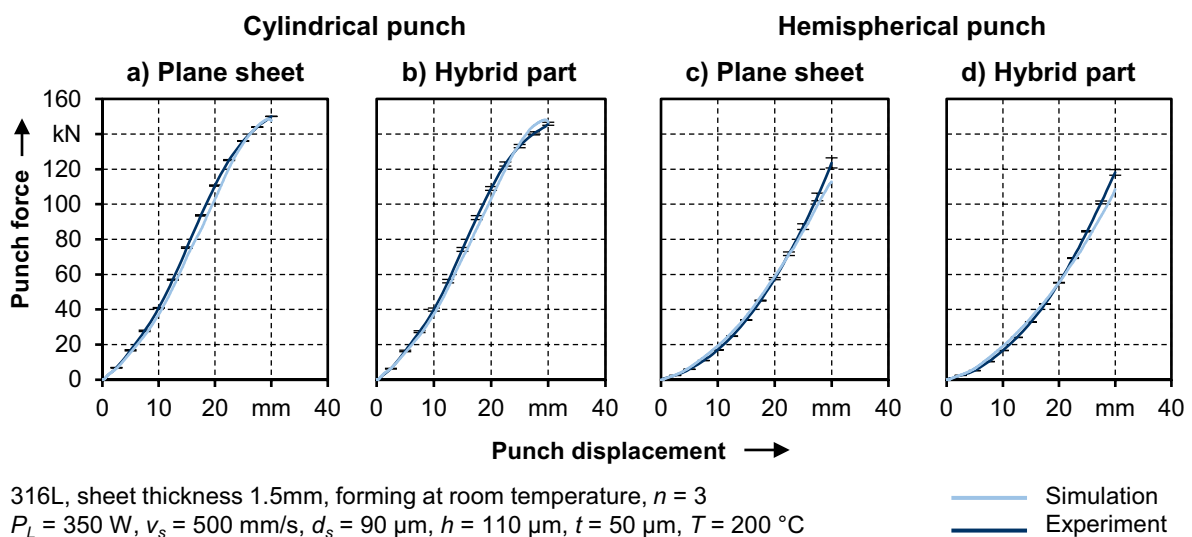


Fig. 6 Force–displacement curves from physical experiments and simulations for deep drawing of plane sheet and hybrid parts

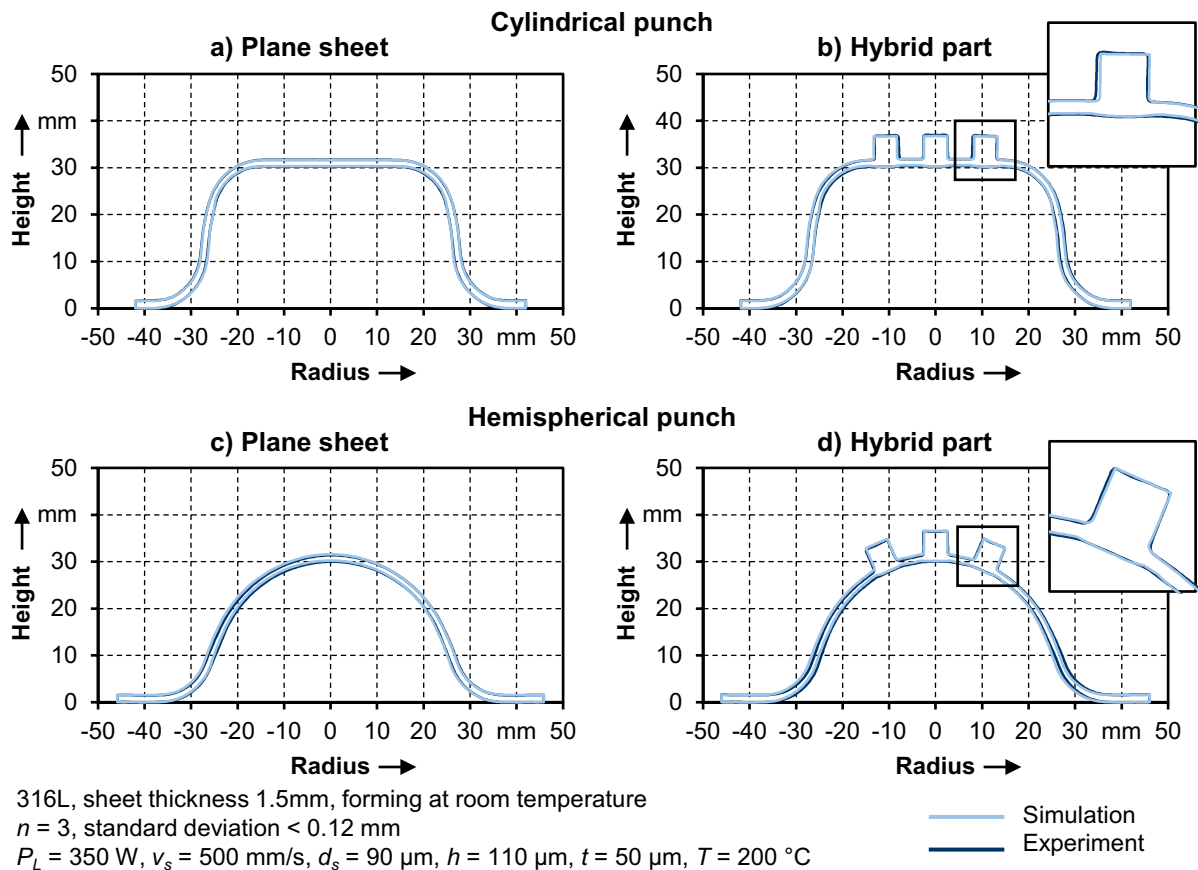


Fig. 7 Comparison of cross sections in rolling direction between numerical simulation and physical experiment for the two investigated punch geometries

state in the forming zone depending on the punch geometry. In the case of cylindrical punches, the forming zone is characterized by tensile-compressive stresses leading to the plastic deformation [30]. The forming force is transferred from the punch into the bottom of the part along the wall into the flange area where the deformation zone is [31]. The different strain states along this way are exemplary shown in Fig. 8. Hemispherical punches lead to a larger amount of tensile stresses in the forming zone [32], thus leading to tensile strains. The intentional thickness reduction of the part is the result of evenly distributed tensile stresses brought into sheet by the punch [31]. The different strain states as a result of the stresses are shown in Fig. 9 for a part formed with hemispherical punch along its radius.

Starting in the middle of the deep drawn part (Fig. 8) and following a radial path, certain strain states are passed. The bottom of the part is characterized by biaxial tensile strains, which increase with the distance to the middle. These strains are lower compared to the forming zone in the flange. This is due to the normal stresses induced by the punch in the center of the part, leading to friction between sheet and tool. As a consequence, the material

flow and thus the strains is limited. At the edge of the bottom, the material is bent around the punch radius twice and also tensed in radial direction. These tensile strains located in the wall of the cup correspond to the plane strain area. By passing the die radius and going to the edge of the part, the strains become tensile-compressive. The material is tensed radially and compressed tangentially and in normal direction. The maximum strains are found in the forming zone close to the die radius. Towards the edge of the part, the strains decrease again. [31]

The strain states of the part drawn with the hemispherical punch (Fig. 9) are distributed from biaxial tensile strains up to tensile-compressive strains as well. But due to the shape of the punch, a larger area in the center of the part is loaded with biaxial tensile stresses. However, the even distribution of these stresses lead to higher strains for each element but lower maximum strains. With further distance to the middle of the part the strains pass the plane strain state and become tensile-compressive in the flange area. Moreover, the strains in the tensile-compressive area are found to be lower in scale as well, but still present.

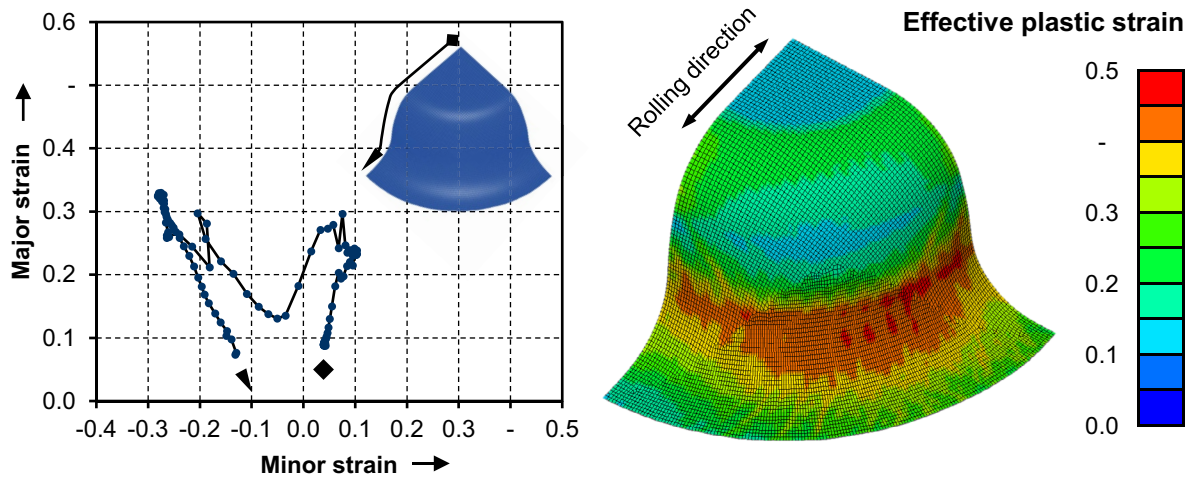


Fig. 8 Strain states along a radial path for a cylindrical punch and the resulting effective plastic strains from a numerical simulation

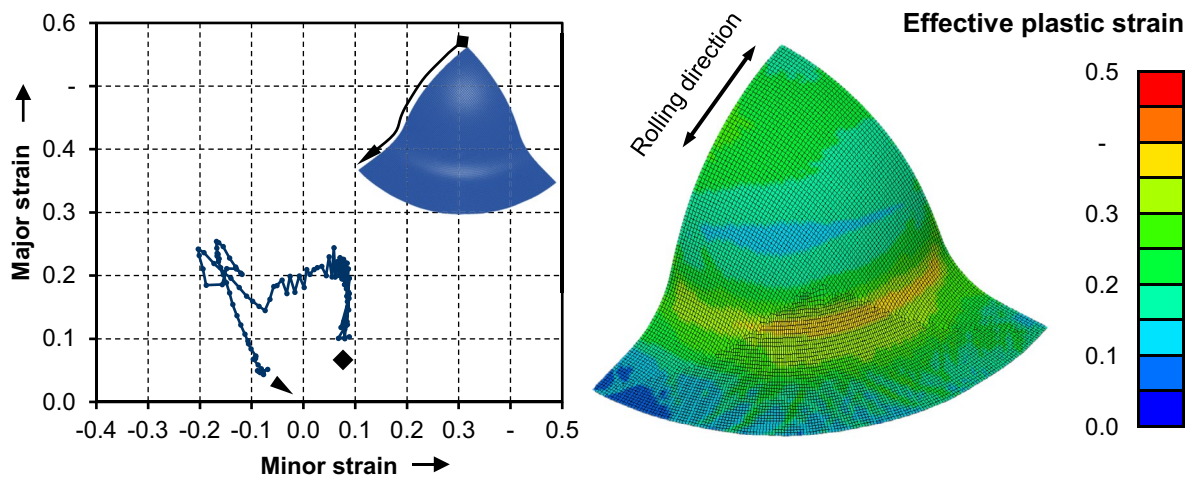


Fig. 9 Strain states along a radial path for a hemispherical punch and the resulting effective plastic strains from a numerical simulation

In comparison, both punch geometries lead to high strains in the area of the die radius due to the high stresses, whereas the strains are higher for the cylindrical shape. An additional area of high strains is found in at the punch radius for both processes. For the cylindrical punch, this area is limited. However, for the hemispherical punch geometry, the loaded area is larger. This area begins in the middle of the part and reaches to the point of contact loss between punch and sheet. The center of the part is of special interest as in the case of hybrid parts, the AMEs are located in this region. For both processes, this area is loaded with biaxial tensile stresses but at different scales. While the area is affected by little loads for the cylindrical punch, the parts formed with hemispherical punch show high loads in the central area.

How the presence of the functional elements influences the forming process is shown in the next sections.

3.3 Influence of the AMEs on sheet metal forming processes

To work out an insight on the influence on the forming process of the stress state the AMEs are located in, the sheet metal forming processes deep drawing and stretch forming are analyzed individually. Afterwards, the results can be compared to conclude the cause-effect correlations. At first, the deep drawing process is compared regarding the forming of a plane sheet and a hybrid part. Secondly, the stretch forming operation is investigated with the same regard.

3.3.1 Influence of the AMEs on deep drawing with cylindrical punch

In order to understand the influence of the AMEs, the different areas of a deep drawn part with the resulting stresses are shown in Fig. 10 for plane sheet. Based on that, first assumptions regarding the interactions can be made.

The deep drawing part is characterized by five distinct areas: cup bottom, punch radius, cup wall, die radius and flange area [13]. The main deformation area is found towards the flange, where the characteristic tensile-compressive stresses are found. Passing the double bending around the punch in the area of the die radius, tensile stresses in radial direction are located in the wall of the cup. Another double bending happens at the punch radius before the bottom of the cup is reached. At this area, biaxial tensile stresses are found, which are usually the lowest over the whole part.

AMEs placed in this location are loaded with the very same stresses. However, due to the low level of stresses and the absence of a bending at the punch radius, the resulting influence is expected to be small.

According to [25], stresses are concentrated at the transition area between sheet metal and AME in forming processes of hybrid parts. Therefore, the resulting stresses are investigated for the plane sheet and the hybrid part in the deep drawing process. The resulting effective stresses are shown in Fig. 11 for both parts as a quarter section of the part.

Analogously to the maximum strains, described in the previous section, the maximum stresses are found at the area of the die radius as well. This is the area, where the tensile stresses in radial direction and the compressive stresses in tangential direction lead to the deformation of the part during the process. Towards the edge, the stresses decrease as

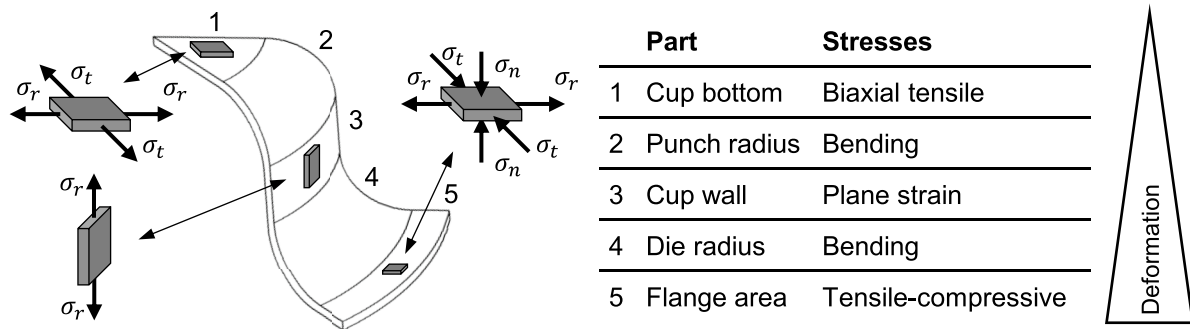


Fig. 10 Different areas of deep drawn parts (cylindrical punch) with the resulting stresses according to [13]

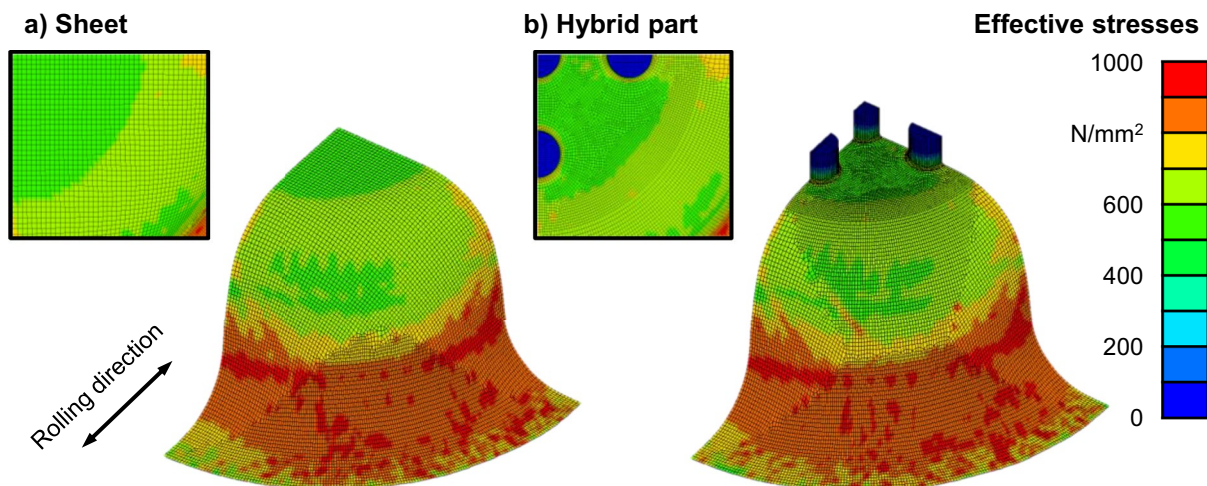


Fig. 11 Effective stresses of deep drawn (cylindrical punch) a sheet and b hybrid part; visualization in quarter section

well as towards the middle of the part, where they are lowest in scale. As a consequence, the presence of the AMEs only leads to a small increase of stresses in radial direction next to the AMEs, which can be seen in the detail of Fig. 11. Still, the increase in stresses is present and can be ascribed to the increased stiffness as a result of the higher “thickness”. To investigate the effect of the AMEs on the geometry of the part, the comparison of contours is shown in Fig. 12.

Overall, the geometry of hybrid part and sheet are almost identical. The only difference is found in the bottom of the cup. The stretching of the sheet, as it happens in the beginning of the process due to the biaxial tensions, leads to a reduction of the sheet’s thickness. For the plane sheet, this is found over the whole bottom area of the cup. However, the hybrid parts exhibit changes in sheet thickness in the same area. Beneath the AME a convex curvature is found, which is oriented towards the punch. This is also found for the titanium hybrid parts in [24], leading to a contact loss (Fig. 12b). Moreover, the hybrid part is “lifted” compared to the conventional sheet (Fig. 12a). Both effects can be attributed to the curvatures on the bottom side of the sheet, shown in Fig. 13.

The convex area is the result of the thermal expansion and contraction caused by the laser’s heat input during the AM process. The peak of this curvature is in the middle of the AME and represents the point, where the sheet is tensed the

least and stays closest to the nominal sheet thickness during forming. With increasing distance to this point, the sheet thickness is reduced similarly to the plane sheet. In contrast to the sheet, the hybrid part’s sheet component does not have full contact to the punch, but is rather placed on top of these curvatures (Fig. 13a). These contact points are visible on the back side of the parts formed in the physical experiments (Fig. 13b). Since the contact between punch and sheet is only present at these points for hybrid parts, the material is free to flow in the surrounding area until the sheet has contact to the punch radius. As a consequence, the stretching in the beginning of the process is higher compared to conventional sheet. This effect is visible in the comparison of the sheet thickness and the resulting sheet thickness reduction between sheet and hybrid part, which is shown in Fig. 14.

In general, the thickness of the sheet and hybrid part are similar and show the common characteristics of deep drawn parts. The thickness in the flange is increased due to the compressive tangential stresses. With the passing of the die radius the material is rather stretched than compressed, which leads to a thickness reduction. The minimum thickness is reached at the punch radius for both parts. Here, the highest reduction of thickness is approximately 20%. Towards the center of the part, the thickness is reduced less again but remains below the initial thickness. The reduced thickness in the center is caused by the biaxial tensile

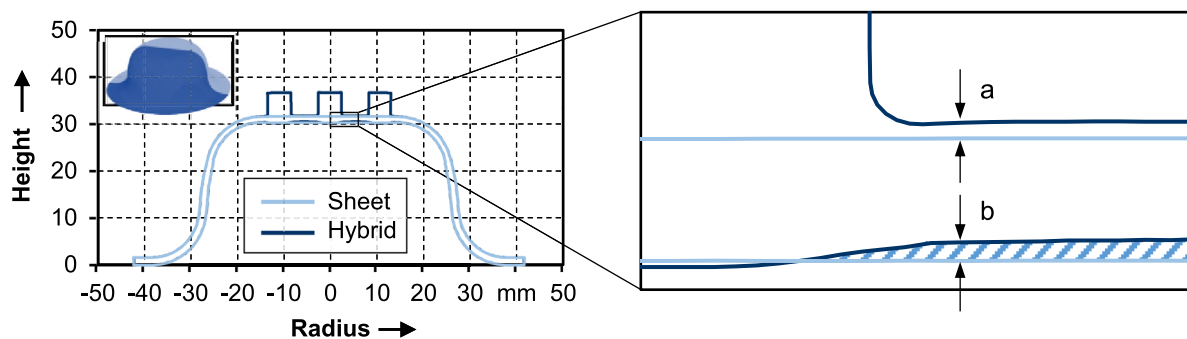


Fig. 12 Contours in rolling direction of deep drawn (cylindrical punch) sheet and hybrid part from the numerical simulation

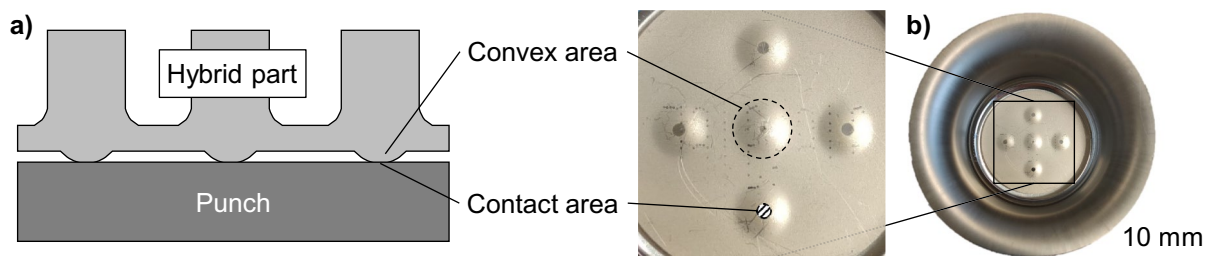


Fig. 13 a Schematic section of hybrid part’s contact to the punch during forming b bottom view of a deep drawn (cylindrical punch) hybrid part with curvatures and contact area

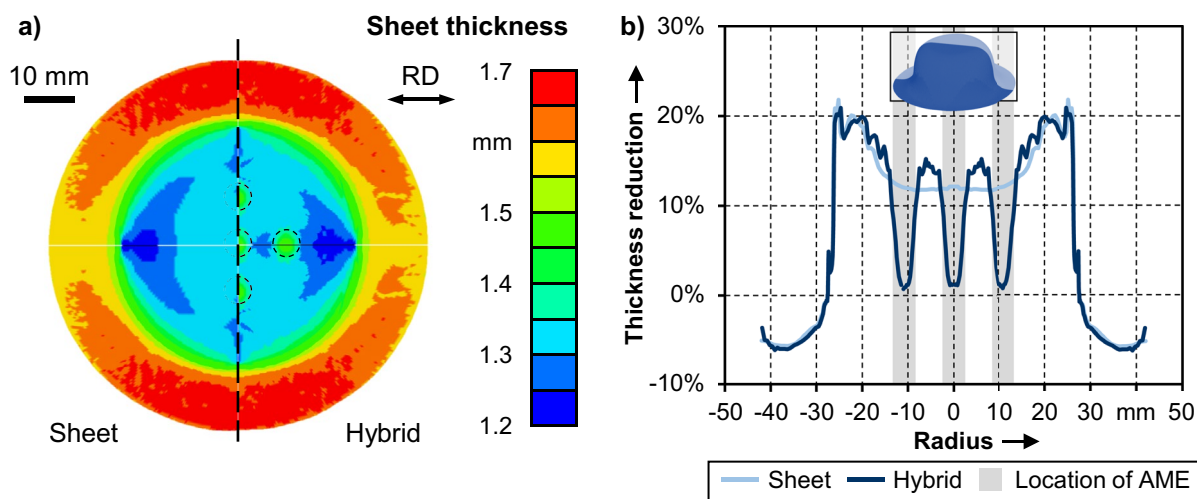


Fig. 14 **a** Thickness distribution and **b** thickness reduction along section parallel to the rolling direction for deep drawn (cylindrical punch) sheet metal and hybrid part from the numerical process simulation

stresses. This area is mostly affected at the beginning of the process and the differences between sheet metal and hybrid part are most prominent there. For the sheet without AMEs, the thickness distribution is even. For the hybrid part however, the sheet thickness fluctuates. Right beneath the AME, the sheet thickness is closest to the initial state. Due to the minimal contact between sheet and the punch (Fig. 13) and the resulting friction, the material flow is reduced. Whereas next to these contact areas, the material is free to flow and thus results in a reduced thickness. Henceforth, the material flow is less limited than for the conventional sheet with the full contact to the punch and the friction over the

whole center of the part. As a result, the thickness reduction between the AMEs of the hybrid part is higher compared to the conventional sheet. These concentrations are found in [24] for stretch formed parts as well. Still, these maxima are lower compared to the ones at the punch radius. Whether this reduction is critical in terms of material failure is investigated by comparing the strain distribution of the elements in the numerical simulation with regard to a forming limit curve (FLC). The resulting strains are shown for both parts in Fig. 15.

In general, the strains of the sheet and the hybrid part are similar. The smaller section found in the area of

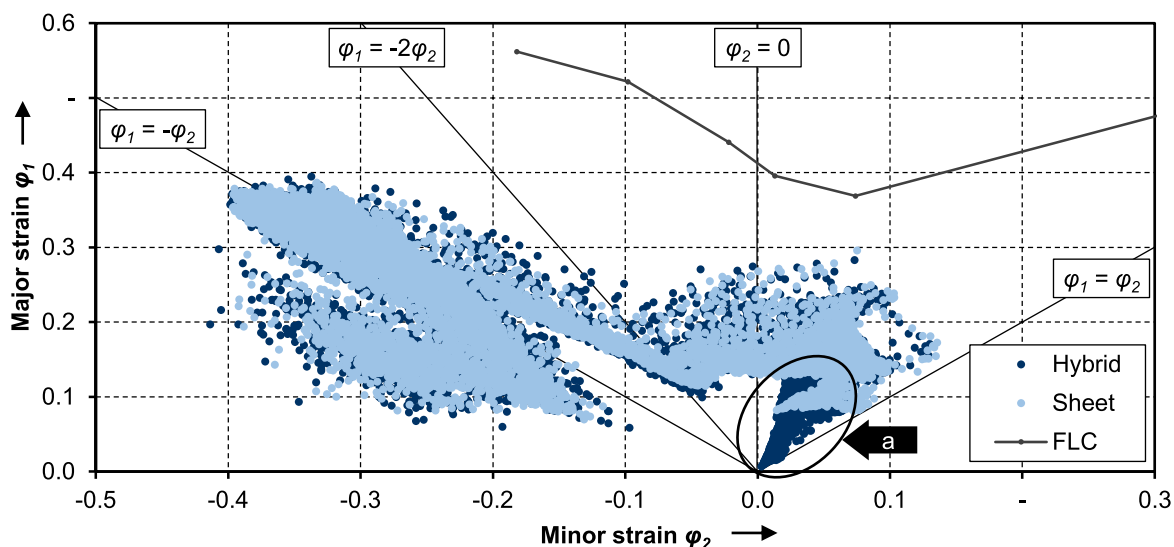


Fig. 15 Major and minor strains from the numerical investigation for deep drawn (cylindrical punch) sheet and hybrid part with FLC and marked area of highest differences (a)

positive major and minor strains corresponds to the bottom of the cup, which is stretch formed. There, biaxial tensile stresses are found. The bigger section is located in the area of negative (compressive) minor strains. With regard to the relation between major and minor strain, this corresponds to the area of uniaxial tension ($\varphi_1 = -2\varphi_2$) or deep drawing ($\varphi_1 = -\varphi_2$). The most critical area in terms of material failure due to fracture is found for positive minor strains close to zero. According to the consistent volume of the material, the sum of the strains in all three directions is equal to zero. This means that for low or zero minor strains, all of the major strains are compensated by a reduction of the sheet thickness. This in turn, leads to the necking of the material and consequently to a fracture. For the highest major strains in the area of low positive minor strains, there is no significant difference between the sheet and the hybrid part. The biggest difference is found for low, positive major and minor strains (Fig. 15a). Derived from the numerical simulation, the “additional” points for the hybrid part correspond to the area beneath the AME, where the deformation is limited. This finding is consistent with the results from the thickness reduction in the previous section.

To summarize, the deep drawing operation of the hybrid parts with cylindrical punch results in altered contact conditions, which influence the material flow. Increased thickness reductions are found in the area common for the deep drawing process (punch radius) and additionally between the AMEs. However, the change in formability and susceptibility to failure due to the presence of AMEs is not incisive for the deep drawing operation. This can be explained by the AMEs being located in the area of the part, which is not in the main deformation zone and therefore less critical. In the next section, the influence of a hemispherical punch is investigated.

3.3.2 Influence of the AMEs on deep drawing with hemispherical punch

Similar to the deep drawing operation with cylindrical punch, the part manufactured with hemispherical punch is characterized by distinct zones with their characteristic stresses. A schematic presentation of the part is shown in Fig. 16.

The absence of a fixed flange area leads to a material flow and thus results in tensile-compressive stresses. At the die radius, the material is bent twice and merges into the plane strain area. The central area is characterized by the tensile biaxial stresses. In contrast to cylindrical punch, the scale of the stresses is higher. Most of the deformation happens in the center and plane strain area. For the hybrid parts, the AMEs are placed in the area of tensile biaxial stresses and thus undergo the same loads. As described in Sect. 3.2, the strains found in the center of the part are higher for the hemispherical punch than for the cylindrical one. This is further increased by the sheet bending around the punch leading to a tilting of the AMEs with respect to the distance from the center. Therefore, a stronger effect of the AME on the forming process and the resulting sheet thickness is expected. To investigate the stress concentrating effect of AMEs in this processes, the sheet and hybrid part are compared regarding the effective stresses. Figure 17 shows the resulting stresses from the numerical simulations.

In accordance with the strains analyzed in Sect. 3.2, stress peaks are found in the area of the die radius as well, for both parts. Again, these peaks are the result of the tensile-compressive stresses in the main deformation zone. Of higher importance are the clearly visible stress concentrations found in the center of the hybrid part (Fig. 17b). The concentrations are located at the transition area between AME and sheet metal, as described in [25] for one AME. As this is a zone of high deformations, a higher influence of the AME is reasonable. The reason for the stress concentrations in the transition area is expected to be due to the differences in

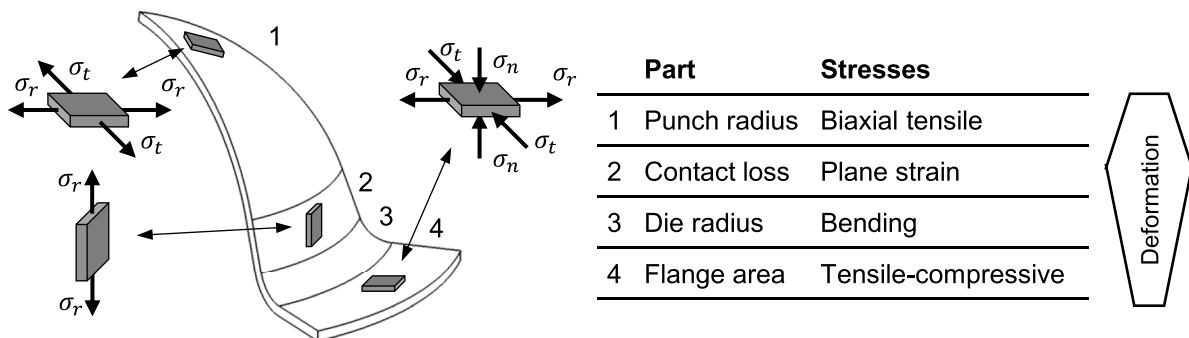


Fig. 16 Different areas and stress states of part deep drawn with hemispherical punch

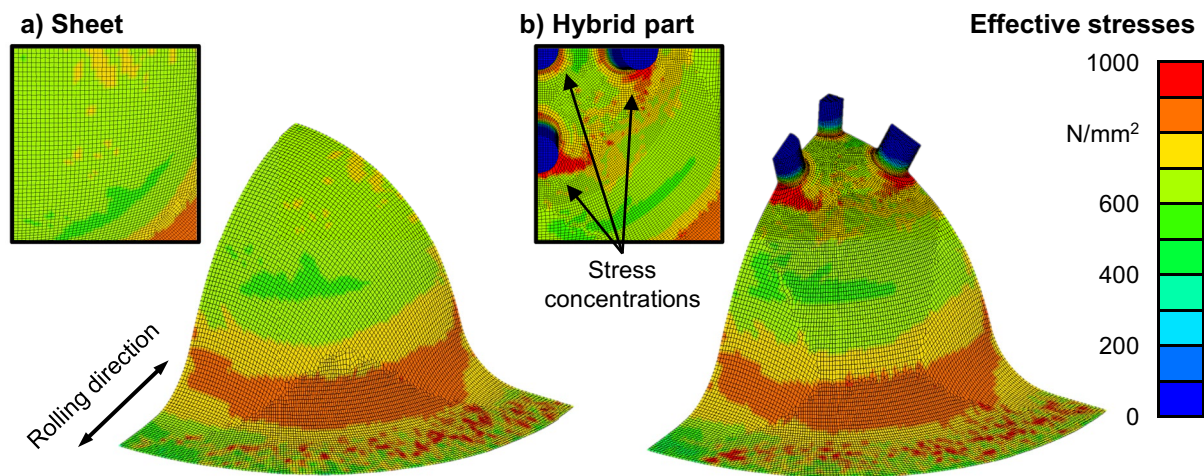


Fig. 17 Effective stresses of deep drawn (hemispherical punch) a) sheet and b) hybrid part; visualization in quarter section

geometry [25], but also due to the contact loss between sheet and punch. Therefore, the geometry of sheet and hybrid part are compared in Fig. 18.

The contour from hybrid part and conventional sheet are almost identical. The biggest difference is found in the center of the part. Similar to the deep drawing process with cylindrical punch, the hybrid part only has contact to the punch directly beneath the AMEs, which is again visible on the parts from the physical experiments. However, the conventional sheet wraps around the punch and thus has full contact. Consequently, the friction is evenly distributed over the part and the material flow is limited. In contrast, the loss of contact between the AMEs of the hybrid part (Fig. 18a) is expected to lead to a free material flow between them and thus to a higher thickness reduction compared to the conventional sheet. On the other hand, the material is bend around the spherical punch, leading to a compression of the sheet in the middle between the AMEs, which is oriented towards the punch (Fig. 18b). As a result, the thickness reduction between the AMEs is lower, which opposes

the general decrease of thickness. This combination leads to bigger gaps between sheet and punch close to the AME and a smaller gap in the middle. To get a better impression of the resulting thickness and the corresponding reduction, the sheet and hybrid part are compared in Fig. 19.

Overall, the thickness distribution of the sheet and the hybrid part are comparable (Fig. 19a). The lowest thickness is found close to the center of the part. Due to the materials anisotropy and the resulting higher strength perpendicular to the rolling direction, the maximum sheet thickness lays in the flange 90° to the rolling direction. Moreover, the minimum sheet thickness is located parallel to the rolling direction due to the lower strength in this direction. Although the AMEs are located in the area of highest thickness reductions, the thickness in the area beneath the AMEs is reduced less compared to the surrounding material. Additionally, the area of reduced thickness of the hybrid part is wider perpendicular to the rolling direction compared to the sheet. When comparing the resulting thickness reduction along the section (Fig. 19b), the highest differences between sheet

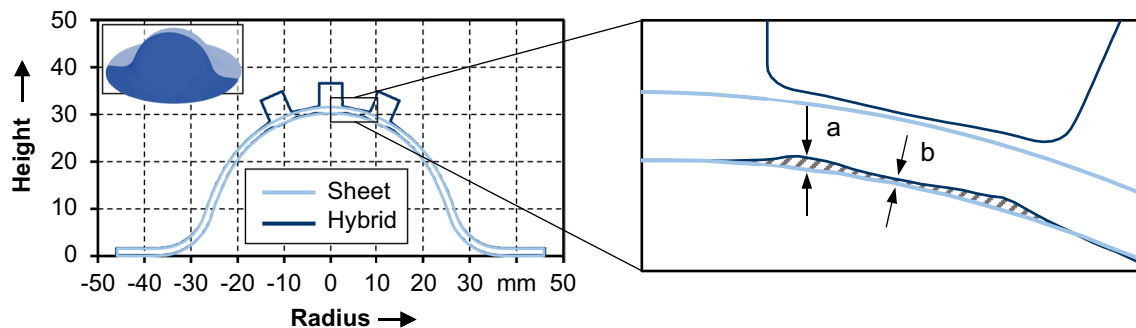


Fig. 18 Contours in rolling direction of deep drawn (hemispherical punch) sheet and hybrid part from the numerical simulation

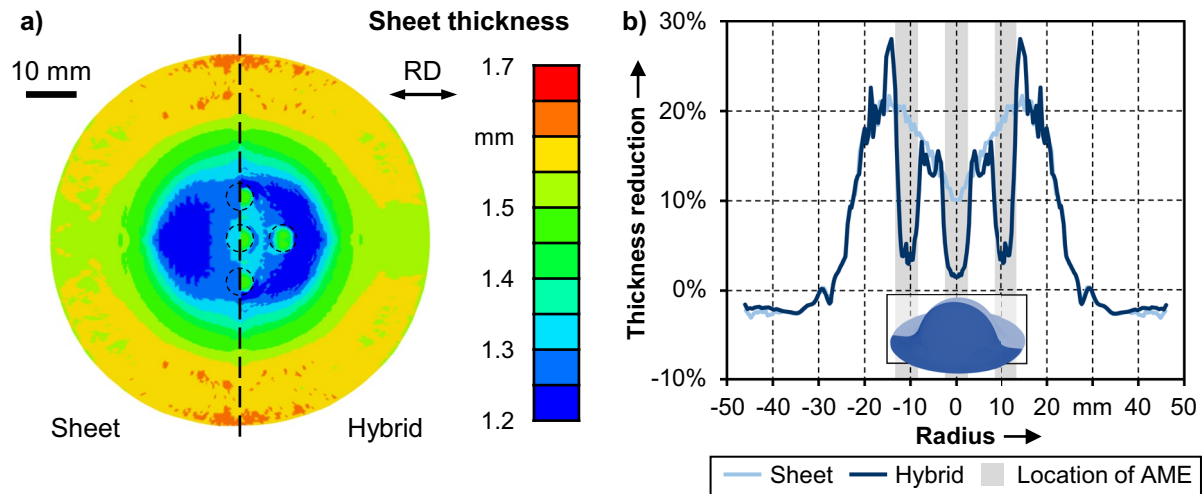


Fig. 19 **a** Thickness distribution and **b** thickness reduction along section parallel to the rolling direction for deep drawn (hemispherical punch) sheet metal and hybrid part from the numerical process simulation

and hybrid part are found for a radius between -20 and 20 mm, as this is the zone of highest deformations and the area where the AMEs are located. Outside of this area, the thickness reductions are almost identical for both parts. For the sheet, the maximum thickness reduction is found at a radius of 15 mm, which is about 21% . Towards the center as well as towards the flange, the thickness is less reduced. The center of the part is the area of first contact between sheet and punch in the process. Thus, there is friction from the start limiting the material flow. With increasing punch displacement, the sheet wraps around the punch and the area with friction caused by contact is increasing. At the edge of this contact area, the material is stretched the most, leading to a constant movement of the stretched area. In contrast to that, the hybrid part's contact to the punch is based on the small areas beneath the AMEs. As a result, the material around the AMEs is free to flow and thus reduced in thickness. Due to the previously mentioned compression of the sheet between the AMEs, the thickness reduction at this point is counteracted partially. At the outer edge of the AMEs however, the maximum thickness reduction is found for the hybrid part. This is also the area, where the sheet has its maximum reduction. Caused by the lack of contact, the thickness reduction is higher for the hybrid part and reaches critical values. Therefore, the formability of sheet and hybrid part is investigated. The resulting strains from the numerical simulation are shown in Fig. 20.

In general, positive (tensile) and negative (compressive) minor strains are found for the formed parts. For negative (compressive) minor strains, the strain distribution of sheet and hybrid part are similar. Since these strains are found in the area of the flange and die radius, the influence of the AMEs is not present there. In contrast to that, the strain

distribution in the range of positive (tensile) minor strains show significant differences. Henceforth, the influence of the AMEs on the material behavior is clearly visible in the center of the part, where the positive major and minor strains are found. The first thing to mention are again the points close to the origin of the diagram (Fig. 20b). These points represent the areas beneath the AMEs, which undergo only little deformations. The second difference is also found for positive minor strains but for major strains above 0.2 (Fig. 20a). The presence of the AMEs leads to a notable increase in major strains. In detail, some of the strains surpass the FLC indicating a material necking or even failure. This can be attributed to the stress concentrating effect of the AME, which results in higher strains i.e. thickness reductions. The reason for the concentrations is found in various aspects. First, the geometry of the hybrid part: the combination of sheet metal with AME on top has a higher resistance towards being formed [23]. Thus, the punch displacement is compensated most by deformations in the area of the sheet without AME [23]. Second, despite the fillet radius, the transition between AME and sheet still results in a stress concentrating effect similar to the results found in [25]. Third, the difference in mechanical properties due to the manufacturing process [24]. Parts produced by additive manufacturing processes usually have a higher strength, among others due to smaller grain sizes as a result of the high cooling rates [33]. However, the hybrid parts formed in physical experiments do not show signs of material failure at a drawing depth of 30 mm. This might be attributed to the heat input of the PBF-LB/M-processes leading to an increase of ductility in the transition area.

Altogether, the deep drawing operation with hemispherical punch is notably influenced by the presence of the AMEs

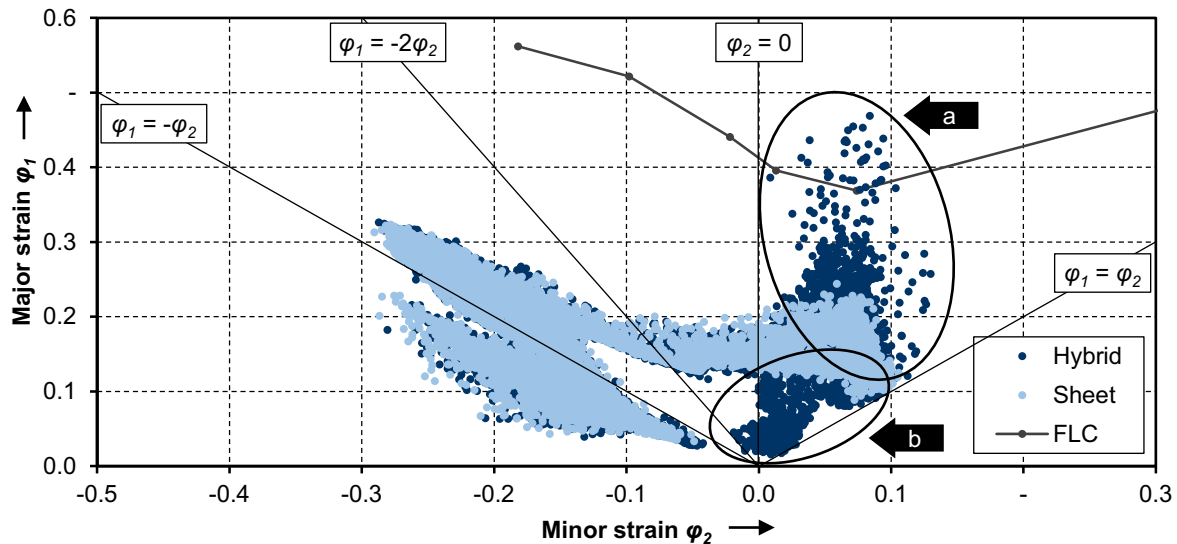


Fig. 20 Major and minor strains from the numerical investigation for deep drawn (hemispherical punch) sheet and hybrid part with FLC and marked areas of highest differences (a) and (b)

due to their positioning in the highly strained central area of the part. The result are stress concentrations, which are caused by the changed contact conditions, the resulting loss of friction and the superposed bending between the AMEs. Consequently, the sheet thickness reduction in the area around the AMEs is higher compared to a conventional sheet, whereas it is partly compensated by the bending. The combination of stress concentration and higher thickness reductions leads to a lowered formability and therefore implies an earlier failure of hybrid parts compared to conventional sheets. The influence of the AME on the forming process is clearly visible. A comparison between the two investigated processes for hybrid parts is found in the next section.

3.4 Comparison of the AMEs' influence on the forming process with regard to the stress state

Regardless of the process, the presence of AMEs influences the process boundary conditions and thus leads to a change of the resulting part properties. The effect found in this investigation for both punch geometries comprises three linked aspects, shown in Fig. 21.

On the opposite side of the AMEs, convex curvatures are found on the bottom of the sheet metal, which are the result of the heat input induced during the PBF-LB/M process. During the forming operation, the curvatures lead to a reduced contact between sheet and punch, as there is only contact at these points (Fig. 21 left). This enables a free material flow between the AMEs. For the process with hemispherical punch, the shape of the punch leads to an

additional bending around the tool (Fig. 21b left). At the same time, the geometry, the sharp transition and the differences in material properties of hybrid parts lead to stress concentrations at the transition between AME and sheet metal (Fig. 21b middle). As a consequence, the sheet is loaded particularly in these areas leading to a necking of the material (Fig. 21 right) and a reduced formability of the whole part.

Although these effects are found for both processes, they affect the parts to a different extent. For the cylindrical punch, the differences found for sheet metal and hybrid part are little. Neither the geometry, nor the resulting thickness reductions show big differences. To summarize, the influence of the AMEs on the deep drawing process is only little. The process with hemispherical punch however is strongly influenced by the AMEs' presence. This is found for the areas with increased stresses, strains and for the highest thickness reductions as well. In fact, the AMEs reduce the process limits since the same drawing depth results in a critical state for the hybrid part, whereas for the sheet metal the strains are still in a safe region. In order to explain the different extents of the influence, the strains are shown for the sheet without AMEs in Fig. 22.

The main deformation zone of the deep drawing process with cylindrical punch is located in the area of the die radius. The AMEs, however, are placed in the center of the part, which corresponds to the bottom of the cup. As shown in Fig. 22a, the strains in this area are among the lowest for the whole part, which can be attributed to the limited material flow and the low biaxial tensile stresses. Stresses and strains in this area may be increased by the presence of the AMEs, but due to their low scale, the

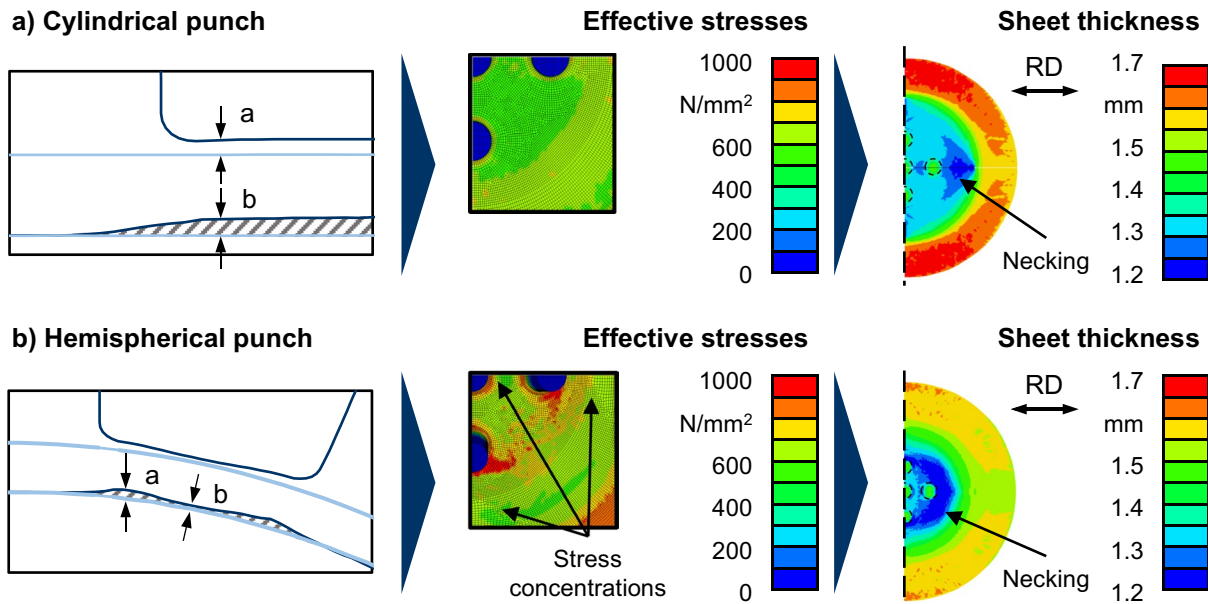


Fig. 21 Three aspects influencing the deep drawing processes for hybrid parts: loss of contact due to lifted sheet metal (left), stress concentrations at transition area (middle), necking in transition area (right)

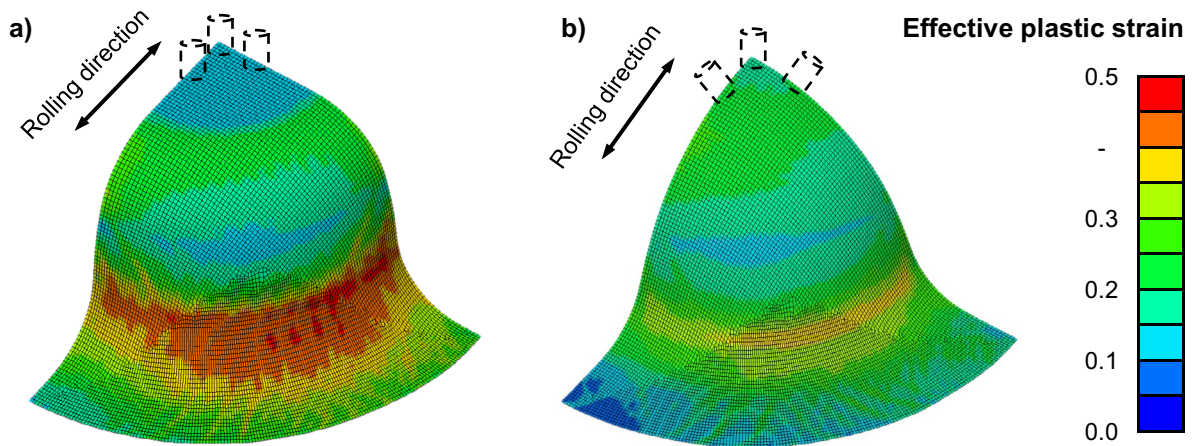


Fig. 22 Effective plastic strains from the numerical simulation of the deep drawing process with **a** cylindrical and **b** hemispherical punch geometry with indicated position of the AMEs

resulting effect is moderately low. In contrast to that, in the central area of the part formed with hemispherical punch, biaxial tensile stresses higher than for the part deep drawn with cylindrical punch are present. An additional bending around the spherical punch as well as the lack of contact lead to higher stresses and accordingly strains compared to the deep drawing part. Therefore, the effect of the AMEs is higher for the operation with hemispherical punch than for the cylindrical one, which is also found in [25] for one AME and titanium parts. Although the AMEs are located in an area characterized by biaxial tensile stress states for

both processes, the degree of influence is significantly different. Whereas the part drawn with cylindrical punch is almost not affected, the part manufactured with hemispherical punch is pushed to the limits. The AMEs lead to the concentration of stresses and strain in the surrounding area. If placed in highly loaded area, the concentrating effect of AMEs is even stronger. In return, areas, which face low deformations, are influenced way less. Under those circumstances, it is best to place AMEs in areas with low stresses and strains, if possible.

4 Summary and outlook

Challenging requirements of current trends in production technologies call for innovative approaches. A promising one is found in the combination of processes to manufacture hybrid parts. One example are hybrid sheets, which combine personalized additive structured and the geometry of sheet metal forming processes. Due to the lack of understanding regarding the interactions during the forming of hybrid sheets, further investigations are required.

By using an analysis combining numerical simulation and experimental results, the understanding of sheet metal forming processes with hybrid parts should be improved. Hybrid parts consisting of sheet metal with additively manufactured elements (AME) made by laser based powder bed fusion are formed in a deep drawing process with two punch geometries to investigate the influence of the additive structures on the process. Within the numerical simulation, a local adapted material modelling approach is used in order to represent the differences of the real parts accurately.

Based on the results of the combined investigations, the AMEs increase stresses and strains. However, the extent of increase depends on the area, in which the AMEs are located. If the area is highly stressed, the concentrating effect is even stronger. Areas with low stresses are only affected to a reduced extent. The concentrating effect was found to be the result of differences in geometry, mechanical properties and the change in contact conditions during forming. Due to the heat input during the additive manufacturing process, the material expands on the backside of the AMEs. The contact between punch and sheet is only present at these curvatures, whereas the remaining material is free to flow.

Further research will be conducted towards the possibility using additive structures as functional elements and at the same time specifically manipulate the material flow during forming. In order to achieve that, different number and geometries of AMEs can be used. Moreover, the influence of the PBF-LB/M process' heat input on the sheet metal of hybrid part is focus of further research in order to improve the numerical simulation.

Author contributions Conceptualization: JH, MM. Methodology: JH, MM. Formal analysis and investigations: JH. Writing—original draft preparation: JH. Writing—review and editing: JH, MM. Funding acquisition: MM. Resources: MM. Supervision: MM.

Funding Open Access funding enabled and organized by Projekt DEAL. Funded by the Deutsche Forschungsgemeinschaft (DFG, German Research Foundation)—Project-ID 61375930—SFB 814—“Additive Manufacturing” TP B05.

Availability of data and material The raw data required to reproduce these findings cannot be shared at this time as the data also forms part of an ongoing study.

Code availability The code required to reproduce these findings cannot be shared at this time as the code also forms part of an ongoing study.

Declarations

Conflict of interest Not applicable.

Open Access This article is licensed under a Creative Commons Attribution 4.0 International License, which permits use, sharing, adaptation, distribution and reproduction in any medium or format, as long as you give appropriate credit to the original author(s) and the source, provide a link to the Creative Commons licence, and indicate if changes were made. The images or other third party material in this article are included in the article's Creative Commons licence, unless indicated otherwise in a credit line to the material. If material is not included in the article's Creative Commons licence and your intended use is not permitted by statutory regulation or exceeds the permitted use, you will need to obtain permission directly from the copyright holder. To view a copy of this licence, visit <http://creativecommons.org/licenses/by/4.0/>.

References

1. Tseng MM, Jiao J (2001) Mass customization. In: Salvendy G (ed) Handbook of industrial engineering. Wiley, Hoboken, pp 684–709. <https://doi.org/10.1002/9780470172339.ch25>
2. Coletti P, Aichner T (2011) Mass customization. Springer Berlin Heidelberg, Berlin, Heidelberg. <https://doi.org/10.1007/978-3-642-18390-4>
3. Lampel J, Mintzberg H (1996) Customizing customization. *Sloan Manag Rev* 38:21–30
4. Lachmayer R, Lippert RB, Kaieler S (2018) Additive serienfertigung. Springer Berlin Heidelberg, Berlin, Heidelberg. <https://doi.org/10.1007/978-3-662-56463-9>
5. Brückner F, Leyens C (2017) Hybrid laser manufacturing. In: Brandt M (ed) Laser additive manufacturing: materials, design, technologies, and applications. Elsevier, Amsterdam
6. Dutta B, Froes FH (2016) Additive manufacturing of titanium alloys: state of the art, challenges, and opportunities. BH Butterworth-Heinemann an imprint of Elsevier, Amsterdam, Boston, Heidelberg, London
7. Gibson I, Rosen D, Stucker B (2015) Additive manufacturing technologies: 3D printing, rapid prototyping and direct digital manufacturing, 2nd edn. Springer, New York, Heidelberg, Dordrecht, London
8. Edwards P, Ramulu M (2014) Fatigue performance evaluation of selective laser melted Ti–6Al–4V. *Mater Sci Eng, A* 598:327–337. <https://doi.org/10.1016/j.msea.2014.01.041>
9. Klocke F, Roderburg A, Zeppenfeld C (2011) Design methodology for hybrid production processes. *Procedia Eng* 9:417–430. <https://doi.org/10.1016/j.proeng.2011.03.130>
10. Pragana JPM, Sampaio RFV, Bragança IMF, Silva CMA, Martins PAF (2021) Hybrid metal additive manufacturing: a state-of-the-art review. *Adv Ind Manuf Eng* 2:1–21. <https://doi.org/10.1016/j.aim.2021.100032>
11. Lauwers B, Klocke F, Klink A, Tekkaya AE, Neugebauer R, McIntosh D (2014) Hybrid processes in manufacturing. *CIRP Ann* 63:561–583. <https://doi.org/10.1016/j.cirp.2014.05.003>

12. Sealy MP, Madireddy G, Williams RE, Rao P, Toursangsarak M (2018) Hybrid processes in additive manufacturing. *J Manuf Sci Eng* 140:79. <https://doi.org/10.1115/1.4038644>
13. Klocke F (2013) *Manufacturing processes: 4: forming*. Springer, Berlin, New York
14. Bambach MD, Bambach M, Sviridov A, Weiss S (2017) New process chains involving additive manufacturing and metal forming—a chance for saving energy? *Procedia Eng* 207:1176–1181. <https://doi.org/10.1016/j.proeng.2017.10.1049>
15. Bambach M, Sviridov A, Weisheit A (2017) Stiffness management of sheet metal parts using laser metal deposition. In: Brabazon D, Naher S, Ahad IU (eds) *Proceedings of the 20th International ESAFORM Conference on Material Forming: ESAFORM 2017*: Dublin, Ireland, 26–28 April 2017. AIP Publishing, Melville, New York, p 80014. <https://doi.org/10.1063/1.5008094>
16. Ambrogio G, Gagliardi F, Muzzupappa M, Filice L (2019) Additive-incremental forming hybrid manufacturing technique to improve customised part performance. *J Manuf Process* 37:386–391. <https://doi.org/10.1016/j.jmapro.2018.12.008>
17. Merklein M, Schulte R, Papke T (2021) An innovative process combination of additive manufacturing and sheet bulk metal forming for manufacturing a functional hybrid part. *J Mater Process Technol* 291:117032. <https://doi.org/10.1016/j.jmatprotec.2020.117032>
18. Ünsal I, Hama-Saleh R, Sviridov A, Bambach M, Weisheit A, Schleifenbaum JH (2018) Mechanical properties of sheet metal components with local reinforcement produced by additive manufacturing. In: Fratini L, Di Lorenzo R, Buffa G, Ingarao G (eds) *Proceedings of the 21st International ESAFORM Conference on Material Forming: ESAFORM 2018*: Palermo, Italy, 23–25 April 2018. AIP Publishing, Melville, New York, p 160028. <https://doi.org/10.1063/1.5035054>
19. Hama-Saleh R, Weisheit A, Schleifenbaum JH, Ünsal I, Sviridov A, Bambach M (2020) Formability analysis of micro-alloyed sheet metals reinforced by additive manufacturing. *Procedia Manuf* 47:1023–1028. <https://doi.org/10.1016/j.promfg.2020.04.317>
20. Merklein M, Dubjella P, Schaub A, Butzhammer L, Schmidt M (2016) Interaction of additive manufacturing and forming. In: Drstvenšek I, Drummer D, Schmidt M (eds) *6th International Conference on Additive Technologies - iCAT 2016: Proceedings: Nürnberg, Germany, 29.-30. November 2016*: DAAAM Specialized Conference. Interesansa - zavod, Ljubljana, pp 309–316
21. Butzhammer L, Dubjella P, Huber F, Schaub A, Aumüller M, Baum A, Petrunenko O, Merklein M, Schmidt M (2017) Experimental investigation of a process chain combining sheet metal bending and laser beam melting of Ti-6Al-4V. In: *Wissenschaftliche Gesellschaft Lasertechnik e.V. (ed) Proceedings of the Lasers in Manufacturing LIM*, Munich
22. Bambach M, Sviridov A, Weisheit A, Schleifenbaum J (2017) Case studies on local reinforcement of sheet metal components by laser additive manufacturing. *Metals* 7:113. <https://doi.org/10.3390/met7040113>
23. Hafenecker J, Papke T, Huber F, Schmidt M, Merklein M (2020) Modelling of hybrid parts made of Ti-6Al-4V sheets and additive manufactured structures. In: Behrens B-A, Brosius A, Hintze W, Ihlenfeldt S, Wulfsberg JP (eds) *Production at the leading edge of technology*. Springer Berlin Heidelberg, Berlin, Heidelberg, pp 13–22. https://doi.org/10.1007/978-3-662-62138-7_2
24. Hafenecker J, Rothfelder R, Schmidt M, Merklein M (2021) Stretch forming of Ti-6Al-4V hybrid parts at elevated temperatures. In: Merklein M, Duflou J, Fratini L, Hagenah H, Martins P, Meschut G, Micari F (eds) *Sheet Metal 2021*. Trans Tech Publications, Limited, Zurich, pp 135–142. <https://doi.org/10.4028/www.scientific.net/KEM.883.135>
25. Hafenecker J, Papke T, Merklein M (2021) Influence of stress states on forming hybrid parts with sheet metal and additively manufactured element. *J Mater Eng Perform* 207:1176. <https://doi.org/10.1007/s11665-021-05674-8>
26. German Institute for Standardization DIN EN 10088-3:2014-12, *Stainless Steels - Part 3: Technical delivery conditions for semi-finished products, bars, rods, wire, sections and bright productions of corrosion resisting steels for general purposes*. Beuth Verlag GmbH, Berlin. <https://doi.org/10.31030/2102108>
27. Heraeus Additive Manufacturing GmbH Metal Powder—Stainless Steel 1.4404/316L. https://www.heraeus.com/media/media/group/doc_group/products_1/additivemanufacturing/datasheets_en/Stainless_Steel_1.4404_316L.pdf. Accessed 10 Feb 2022
28. Barlat F, Brem JC, Yoon JW, Chung K, Dick RE, Lege DJ, Pourboghrat F, Choi S-H, Chu E (2003) Plane stress yield function for aluminum alloy sheets—part 1: theory. *Int J Plast* 19:1297–1319. [https://doi.org/10.1016/S0749-6419\(02\)00019-0](https://doi.org/10.1016/S0749-6419(02)00019-0)
29. Hockett JE, Sherby OD (1975) Large strain deformation of polycrystalline metals at low homologous temperatures. *J Mech Phys Solids* 23:87–98. [https://doi.org/10.1016/0022-5096\(75\)90018-6](https://doi.org/10.1016/0022-5096(75)90018-6)
30. German Institute for Standardization (2003) *Manufacturing processes forming under combination of tensile and compressive conditions—part 1: general—classification, subdivision, terms and definitions*. Beuth Verlag GmbH, Berlin 01.040.25; 25.020; 25.120.20. <https://doi.org/10.31030/9500650>
31. Lange K (ed) (1990) *Umformtechnik: handbuch für industrie und wissenschaft: Band 3: blechbearbeitung, 2., völlig neubearb. und erw. Aufl.* Springer, Berlin
32. German Institute for Standardization *Manufacturing processes forming under tensile conditions—Part 1: General—classification, subdivision, terms and definitions*. Beuth Verlag GmbH, Berlin 01.040.25; 25.020; 25.120.99. <https://doi.org/10.31030/9500657>
33. Frazier WE (2014) Metal additive manufacturing: a review. *J Mater Eng Perform* 23:1917–1928. <https://doi.org/10.1007/s11665-014-0958-z>

Publisher's Note Springer Nature remains neutral with regard to jurisdictional claims in published maps and institutional affiliations.